Available online at www.sciencedirect.com

ScienceDirect

Tectonophysics 448 (2008) 33–48

TECTONOPHYSICS

www.elsevier.com/locate/tecto

Peri-equatorial paleolatitudes for Jurassic radiolarian cherts of Greece

I.W. Aiello [a,*], J.T. Hagstrum [b], G. Principi [c]

[a] *Moss Landing Marine Laboratories, 8272 Moss Landing Road, Moss Landing, CA 95039, USA*
[b] *U.S. Geological Survey, Menlo Park, CA 94025, USA*
[c] *Earth Sciences Department, University of Florence, Florence 50121, Italy*

Received 12 June 2007; received in revised form 8 November 2007; accepted 21 November 2007
Available online 31 December 2007

Abstract

Radiolarian-rich sediments dominated pelagic deposition over large portions of the Tethys Ocean during middle to late Jurassic time as shown by extensive bedded chert sequences found in both continental margin and ophiolite units of the Mediterranean region. Which paleoceanographic mechanisms and paleotectonic setting favored radiolarian deposition during the Jurassic, and the nature of a Tethys-wide change from biosiliceous to biocalcareous (mainly nannofossil) deposition at the beginning of Cretaceous time, have remained open questions. Previous paleomagnetic analyses of Jurassic red radiolarian cherts in the Italian Apennines indicate that radiolarian deposition occurred at low peri-equatorial latitudes, similar to modern day deposition of radiolarian-rich sediments within equatorial zones of high biologic productivity. To test this result for other sectors of the Mediterranean region, we undertook paleomagnetic study of Mesozoic (mostly middle to upper Jurassic) red radiolarian cherts within the Aegean region on the Peloponnesus and in continental Greece. Sampled units are from the Sub-Pelagonian Zone on the Argolis Peninsula, the Pindos–Olonos Zone on the Koroni Peninsula, near Karpenissi in central Greece, and the Ionian Zone in the Varathi area of northwestern Greece. Thermal demagnetization of samples from all sections removed low-temperature viscous and moderate-temperature overprint magnetizations that fail the available fold tests. At Argolis and Koroni, however, the cherts carry a third high-temperature magnetization that generally exhibits a polarity stratigraphy and passes the available fold tests. We interpret the high-temperature component to be the primary magnetization acquired during chert deposition and early diagenesis. At Kandhia and Koliaky (Argolis), the primary declinations and previous results indicate clockwise vertical-axis rotations of ~40° relative to "stable" Europe. Due to ambiguities in hemispheric origin (N or S) and thus paleomagnetic polarity, the observed declinations could indicate either clockwise (CW) or counterclockwise (CCW) vertical-axis rotations. Thus at Adriani (Koroni), the primary declinations indicate either CW or CCW rotations of ~95° or ~84°, depending on paleomagnetic polarity and age. The primary inclinations for all Peloponnesus sites indicate peri-equatorial paleolatitudes similar to those found for coeval radiolarian cherts exposed in other Mediterranean orogenic belts. Our new paleomagnetic data support the interpretation that Mesozoic radiolarites within the Tethys Ocean were originally deposited along peri-equatorial belts of divergence and high biologic productivity.

Keywords: Radiolarian Chert; Jurassic; Paleolatitude; Greece; Paleo-equator

1. Introduction

Radiolarian cherts of Mesozoic (mostly middle to late Jurassic) age are common pelagic deposits found within the tectonic units of Mediterranean orogenic belts. These biosiliceous sediments covered large portions of the Tethys Ocean's deepest basins, and their diagenetic products are a variety of well-bedded siliceous rocks called "radiolarian cherts". The bedding of radiolarian cherts is typically rhythmic and characterized by regular alternations between chert beds and claystone interbeds that might record primary variations in radiolarian plankton productivity. Because of the perplexing abundance of radiolarian chert facies in both continental margin and ophiolite units of the Mesozoic Tethys Ocean, the origins of these ancient biosiliceous deposits have been inferred from a number of different paleoceanographic and paleotectonic models. In an early model, Bosellini and Winterer (1975), Winterer and Bosellini (1981), Barrett (1982), and Jenkins and Winterer (1982), proposed that the accumulation of biosiliceous radiolarian sediments resulted from unusually shallow

* Corresponding author. Tel.: +1 831 771 4480.
E-mail address: iaiello@mlml.calstate.edu (I.W. Aiello).

0040-1951/$ - see front matter © 2007 Elsevier B.V. All rights reserved.
doi:10.1016/j.tecto.2007.11.036

calcium-carbonate compensation depths (CCD) during the Jurassic (~2500 m). Conversely, the distribution of modern biosiliceous sedimentation indicates that high biologic productivity, associated with upwelling of nutrient-rich waters, was a likely requirement for deposition and preservation of radiolarian-rich sediments (e.g., Garrison 1974; Baumgartner, 1987).

Radiolarian cherts are also characteristic of Mesozoic tectonic units in the mountains of Greece (Hellenides). Together with the Dinarides and the Albanides, the Hellenides form a continuous mountain chain that borders the Adriatic and Ionian Seas. This orogenic belt is composed of several NW–SE trending nappes, separated by mostly west-directed thrust sheets, and includes five of the tectono-stratigraphic "zones" recognized by Aubouin (1958) and Aubouin et al. (1970); from top to bottom: (Sub-) Pelagonian, Pindos–Olonos, Gavrovo–Tripolitza, Ionian, and (Pre-) Apulian (Fig. 1). These zones consist of both continental margin and oceanic remnants of the Tethys Ocean, a Triassic seaway that formed after breakup of the Pangea supercontinent. The birth, tectonic evolution, and closure of Tethys are generally ascribed to relative movements between the African and Eurasian plates, and to the complex interplay between intervening oceanic branches and microplates whose number, location, and post-Triassic translational and rotational movements are still a matter of debate (cf. Abbate et al., 1986; Channell, 1996; Robertson et al., 1996; Channell and Kozur, 1997; Aiello and Hagstrum, 2001).

More recent geologic, tectonic, and biostratigraphic investigations of the eastern Mediterranean region, together with an increasing number of paleomagnetic studies, however, have significantly improved our understanding of the paleogeographic origins of rocks within the region's orogenic belts. We now have a more detailed picture of the relative movements between Africa and Eurasia during the Mesozoic, and of vertical-axis rotations and latitudinal displacements within the tectono-stratigraphic units of the region (Turnell, 1988; Channell, 1992; Channell et al., 1992; Morris, 1995; Channell, 1996; Besse and Courtillot, 2002, 2003). Moreover, the lack of detailed age data from Mesozoic units of the Aegean region has in recent years been improved by extensive biostratigraphic studies of pelagic rocks, particularly radiolarian cherts, associated with both continental margin and basaltic units (Baumgartner, 1985; Baumgartner et al., 1995; Chiari, 2001; Bortolotti et al., 2002, 2003).

In the Aegean region, the subjects of most paleomagnetic studies have been Cenozoic, Pliocene, and Pleistocene sedimentary and volcanic rocks exposed across continental Greece, on the Peloponnesus, and in the Greek Islands (e.g. Laj et al., 1982; Kissel and Laj, 1988; Mauritsch et al., 1995; Kondopoulou, 2000; Duermeijer et al., 2000; Kissel et al., 2003; van Hinsbergen et al., 2005a). The reported paleomagnetic directions indicate clockwise (CW) vertical-axis rotations of various degrees, and an overall middle Miocene, and younger, ~50° CW rotation of large sectors of western Greece. These large-scale CW rotations have been linked to episodes of Miocene extension related to the exhumation of metamorphic core complexes and to the formation of Mio–Pliocene extensional basins across continental Greece and the southern Aegean domain. West–southwest motion of the Anatolian

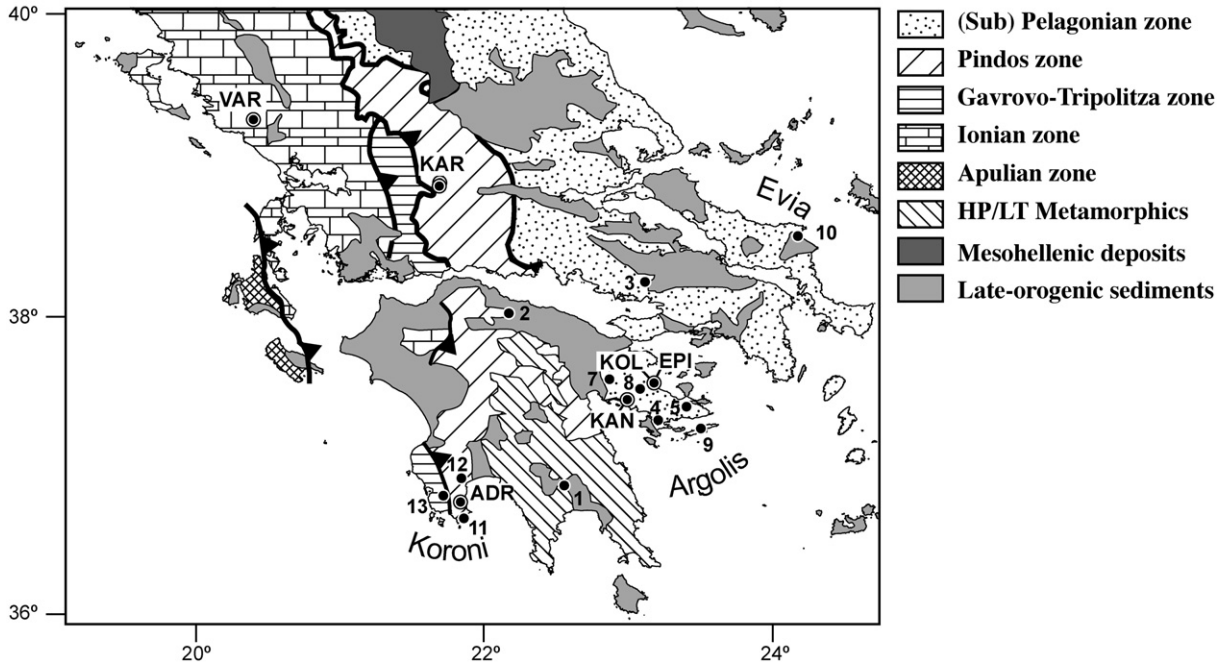

Fig. 1. Structural sketch of Greece and location of the radiolarian chert sections sampled for paleomagnetic analysis (redrawn from van Hinsbergen et al., 2006): Koliaky (KOL; 37.639°N, 23.159°E); Kandhia (KAN; 37.530°N, 22.984°E); Palea Epidavros (EPI; 37.639°N, 23.159°E); Adriani (ADR; 36.867°N, 21.893°E); Karpenissi (KAR; locality I, 38.927°N, 21.754°E; locality II, 38.949°N, 21.757°E); and Varathi (VAR; 39.362°N, 20.538°E). The figure also shows the location of previous paleomagnetic studies discussed in the text (Localities/Age/Reference): 1/Pliocene (Laj et al., 1982); 2/Middle to Upper Cretaceous (Morris, 1995); 3/Oxfordian (Morris, 1995); 4/Middle Jurassic (Pucher et al., 1974); 5/Toarcian to Middle Jurassic (Morris, 1995); 7/Middle Jurassic (Surmont, 1989); 8/Trias (Morris, 1995); 9/Trias (Muttoni et al., 1997); 10/Miocene (Morris, 1995); 11/Plio–Pleistocene (van Hinsbergen et al., 2005a); 12/Plio–Pleistocene (van Hinsbergen et al., 2005a); 13/lower Oligocene (van Hinsbergen et al., 2005a).

tectonic block and northward underthrusting of the African plate beneath the Aegean Sea probably caused the CW rotations (Kissel et al., 2003; van Hinsbergen et al., 2005b).

Increasing paleomagnetic and paleoceanographic evidence from the western Mediterranean region indicates that Jurassic Tethyan radiolarites were deposited on oceanic crust and deep-water continental margins in an east–west-trending zone of high productivity located at peri-equatorial latitudes between Africa and Eurasia (Aiello and Hagstrum, 2001; Muttoni et al., 2005). Paleomagnetic studies of Mesozoic radiolarian cherts in the Italian Alps and Northern Apennines (Aiello and Hagstrum, 2001; Muttoni et al., 2005), along the western margin of North America (Hagstrum and Murchey, 1993; Hagstrum et al., 1996), and in Japan (Shibuya and Sasajima, 1986) have shown that these cherts are well suited for paleomagnetic investigations. Because of their unique lithologic characteristics they alone often preserve primary magnetizations in overprinted terrains that can be successfully isolated using detailed thermal demagnetization procedures.

Reliable paleomagnetic directions, however, have been found by few studies of Mesozoic rocks in Greece (see review by Kondopoulou, 2000). Mesozoic paleomagnetic directions for the Peloponnesus are mostly from Triassic and lower to Middle Jurassic sedimentary rocks of the Sub-Pelagonian Zone that are exposed on the Argolis Peninsula and the Island of Hydra (Turnell, 1988; Muttoni et al., 1994; Morris, 1995). Previous to this study, no paleomagnetic data have been gathered from radiolarian cherts of the Sub-Pelagonian Zone on the Argolis peninsula or the Pindos–Olonos Zone on the Koroni peninsula.

2. Geologic setting

In many paleotectonic reconstructions, the Aegean region is viewed as an accretionary wedge formed by progressive southward stacking of the (Sub-) Pelagonian, Pindos–Olonos, Gavrovo–Tripolitza, and Ionian Zones, with orogenesis having occurred in two main phases (e.g., Feinberg et al., 1996; van Hinsbergen et al., 2005a, and references therein). The Late Jurassic "Eo-Hellenic" phase was caused by obduction of the Pelagonian and Sub-Pelagonian ophiolite units and by widespread emplacement of granites in the Phanos and Monopigadhon units of the Pelagonian Zone (Fig. 1). The second Eocene "Meso-Hellenic" orogenic phase was associated with southerly-directed thrust emplacement in the Axios and Vardar regions, and with underthrusting of the Pindos Zone and Gavrovo–Tripolitza Zone beneath the Sub-Pelagonian Zone (van Hinsbergen et al., 2005c). Regional metamorphic events (e.g., HP/LT of the south Aegean core complex; Jolivet et al., 1996) accompanied the latter orogenic phase, as did formation of the Meso-Hellenic basin since the Late Eocene (Fig. 1; Avramidis et al., 2002). Following the "Meso-Hellenic" orogenesis, western Greece was subjected to two main pulses of late orogenic exhumation and extension in the early Miocene (Jolivet et al., 1996; Jolivet et al., 2003; van Hinsbergen et al., 2005c), with detachment faulting and exhumation of the south Aegean core complex on the Peloponnesus and Crete (Ring et al., 2001), and in late Miocene to early Pliocene time by collision of northern Greece with the Apulian platform and continued subduction of oceanic lithosphere in the Ionian basin beneath southern Greece (van Hinsbergen et al., 2006). In western Greece, compression and large-scale CW rotations, however, were dominant during the intervening middle to late Miocene phase of internal shortening (van Hinsbergen et al., 2006).

Within continental margin units of the Sub-Pelagonian Zone of Argolis, Jurassic pelagic sediments unconformably overlie shallow-water carbonate platforms of Triassic age (Fig. 1; Baumgartner, 1985). These pelagic sediments are typical deep-water facies of the Jurassic Tethys Ocean, and include layers of Ammonitico Rosso limestones and beds of radiolarian cherts. Within most Tethyan continental margin and ophiolite units, Jurassic radiolarian cherts are overlain by early Cretaceous nannofossil-rich limestones (e.g., Vigla Limestones in the Pindos–Olonos Zone, and Maiolica, Biancone and Calpionella Limestone Formations in Italy), but in the Sub-Pelagonian Zone of Argolis the cherts are overlain by Upper Jurassic breccia and flysch deposits. These coarse sediments possibly record early involvement of the Argolis continental margin in the Late Jurassic Eo-Hellenic orogenetic phase (Baumgartner, 1985).

The continental margin units of the Pindos–Olonos Zone exposed on the Koroni Peninsula of the western Peloponnesus are lithologically similar to other units of this zone in southern and central continental Greece (Fig. 1). On both the Koroni Peninsula and near Karpenissi in central Greece, the Pindos–Olonos Zone structurally overlies the Oligocene Flysch units of the Gavrovo–Tripolitza Zone (Fig. 1; Richter et al., 1978). The radiolarian cherts represent deep-water facies of a sedimentary pile that includes Triassic shallow-water carbonate platforms and the clay-rich Pélite de Kasteli Formation (Lower Jurassic; De Wever and Thiébault, 1981). De Wever and Thiébault (1981) estimate that radiolarian cherts exposed on the Koroni Peninsula were deposited between late Jurassic and late Cretaceous time. Radiolarian cherts of the Pindos–Olonos Zone exposed near Karpenissi, however, have a more constrained middle to late Jurassic age (Bajocian to Tithonian; De Wever and Cordey, 1986) and are overlain by the Calpionella Limestone Formation of Tithonian to Berriasian age (Fleury, 1980).

The Ionian Zone is the westernmost of Aubouin's tectono-stratigraphic zones (Fig. 1), and contains no radiolarian chert facies. Radiolarian-rich sediments, however, are concentrated in the middle to upper Jurassic slope sediments of the upper 'Posidonia' beds (Baumgartner et al., 1993), which are part of a sedimentary pile ranging from shallow-water limestones of Triassic (Pantokrator Limestones) and Middle Jurassic age to the deep-water Calpionella Limestone Formation of upper Jurassic to early Cretaceous age.

3. Previous paleomagnetic work in Greece

The following is a synthesis of paleomagnetic work done on the Peloponnesus and in continental Greece that is relevant to our study. For a complete review of paleomagnetic data for Greece refer to van Hinsbergen et al. (2005a), Duermeijer et al. (2000), and Kondopoulou (2000).

Paleomagnetic directions for sediments of Pliocene age on the Peloponnesus (Laj et al., 1982) indicate CW rotations of 9°±8° (I=47.3°, D=12.6°, N=5, k=75, α_{95}=8.9°; Fig. 1, locality 1) relative to stable Europe (*note*: all rotations reported in this section

Table 1
Paleomagnetic data for chert sections in Greece

Sample	Level	I_i	D_i	Strike/dip	I_c	D_c	N	T_{low},T_{high}	λ_{VGP}	ϕ_{VGP}
	(m)	(°)	(°)	(°)/(°)	(°)	(°)		(°C,°C)	(°N)	(°E)
Argolis Peninsula										
Koliaky section										
Component B										
G9001	0.37	−3.2	228.8	328/66	61.4	218.5	2	300,515	32.6	140.0
G9002	0.54	−26.5	227.5	328/74	46.3	224.4	2	300,533	41.8	129.4
G9003	0.58	−13.0	228.7	330/63	48.5	223.5	2	310,530	36.2	135.7
G9004	0.78	7.1	259.0	346/72	78.7	271.4	1	405,530	6.5	122.7
G9005	0.85	11.4	236.3	323/57	68.2	241.7	2	202,533	22.1	139.8
G9006	0.18	−7.0	240.6	344/72	61.7	225.0	2	310,536	25.2	129.2
G9007	2.06	3.7	227.1	333/85	74.1	157.1	2	302,533	31.3	144.2
G9008	2.44	−9.4	219.0	338/87	58.6	181.5	2	408,531	41.6	146.1
G9010	5.95	−1.1	65.1	334/72	−73.1	67.8	1	313,536	19.1	129.4
Average		−4.0	234.7				9		28.6	134.8
Component C										
G9001	0.37	78.3	232.1	328/66	35.6	59.5	2	533,633	35.8	114.9
G9002	0.54	−87.5	268.2	328/74	−13.8	239.3	2	533,633	28.4	127.2
G9003	0.58	−79.5	286.2	330/63	−19.5	248.0	2	550,651	23.5	118.6
G9004	0.78	61.2	5.1	346/72	6.9	48.7	1	637,651	34.0	138.4
G9005	0.85	−65.4	204.1	323/57	−10.9	221.2	1	590,618	40.7	143.3
G9006	0.18	84.5	5.9	344/72	15.9	68.7	2	550,651	21.8	119.8
G9007	2.06	78.2	343.5	333/85	2.7	51.2	2	571,633	30.7	138.2
G9008	2.44	−85.3	173.5	338/87	−1.7	243.5	1	549,569	21.3	129.4
G9010	5.95	−68.6	24.4	334/72	−33.7	260.2	1	536,594	18.7	103.9
Average (NE)					15.3	56.8	4		30.9	128.3
Average (SW)					−16.3	241.9	5		27.2	124.2
Average					15.9	59.6	9		28.9	126.0
Kandhia section										
Component B										
G9020	0.00	−26.7	252.4	103/43	−39.7	281.1	2	208,510	22.4	112.0
G9019	0.03	−20.5	242.5	95/47	−37.4	268.7	2	200,511	28.2	121.5
G9021	0.12	−4.1	233.5	93/48	−31.3	247.2	2	105,552	29.5	135.5
G9022	0.20	−10.6	220.0	93/41	−40.8	234.4	1	200,507	41.4	144.4
G9023	2.26	−5.9	281.8	84/41	7.0	281.4	1	200,536	−7.5	103.4
G9032	3.50	−24.0	259.7	81/37	−19.7	275.0	2	105,512	15.7	109.0
G9025	3.65	−21.9	238.1	84/41	−33.2	259.8	2	200,507	32.1	123.8
G9027	4.80	−9.1	258.9	84/41	−10.2	266.2	2	105,514	11.5	116.1
G9028	7.75	−3.9	246.4	84/41	−14.4	253.1	2	206,512	19.8	126.3
G9033	7.79	5.7	271.7	81/37	11.0	266.1	2	200,539	−3.1	114.2
Average		−12.7	250.5				10		19.3	119.9
Component C										
G9020	0.00	43.2	246.5	103/43	11.8	229.8	2	536,594	26.5	144.9
G9019	0.03	39.4	264.6	95/47	19.3	238.7	2	488,571	17.5	141.0
G9021	0.12	32.9	270.1	93/48	19.4	245.7	2	552,609	12.5	136.2
G9022	0.20	27.7	229.5	93/41	−2.8	223.0	1	507,536	36.5	145.0
G9023	2.26	−9.9	31.7	84/41	22.4	34.7	2	554,572	49.6	143.6
G9030	2.74	−23.0	54.4	84/41	0.2	47.2	2	314,512	32.7	142.3
G9024	2.89	−8.1	48.1	87/40	17.0	50.7	2	647,664	36.1	131.9
G9032	3.50	40.7	251.0	81/37	26.2	227.3	1	512,597	22.2	152.6
G9025	3.65	27.4	232.3	84/41	2.4	223.1	2	572,632	34.5	147.0
G9027	4.80	33.3	281.3	84/41	35.3	251.8	2	414,599	1.7	139.4
G9033	7.79	21.7	264.8	81/37	19.4	250.4	2	539,618	9.0	133.0
Average (SW)					16.7	235.7	8		20.6	142.2
Average (NE)					13.3	44.4	3		39.4	139.0
Average					8.6	232.6	11		25.8	141.4
Palea Epidavros section										
Component C(?)										
G9011	0.01	23.5	47.7	34/20	17.5	54.9	2	504,569	40.6	131.0
G9013	0.50	−15.6	235.9	34/20	−7.5	239.7	1	509,643	26.0	129.7
G9015	1.20	−14.2	252.7	34/20	−1.3	254.8	2	536,659	18.1	118.0
G9016	1.93	−4.6	261.7	34/20	10.2	261.0	2	412,659	8.0	116.4
G9017	2.83	−34.3	284.7	34/20	−15.2	287.6	1	633,646	8.9	96.1
Average					−6.6	255.4	5		13.6	119.5

Table 1 (*continued*)

Sample	Level (m)	I_i (°)	D_i (°)	Strike/dip (°)/(°)	I_c (°)	D_c (°)	N	T_{low},T_{high} (°C,°C)	λ_{VGP} (°N)	ϕ_{VGP} (°E)
Koroni Peninsula										
Adriani section[a]										
Component B										
G9037	4.20	52.6	26.4	339/38	20.5	43.0	1	412,646	68.1	113.7
G9040	8.50	50.2	354.1	353/47	31.0	34.7	1	412,557	82.3	243.3
G9044	11.40	35.0	11.0	355/37	18.8	28.7	1	555,630	70.0	170.2
G9047	14.55	35.5	352.5	342/39	21.0	13.0	2	310,645	71.5	224.6
G9049	15.75	35.2	341.7	348/43	28.9	10.0	2	394,587	66.3	249.4
G9050	16.90	31.2	13.3	353/36	14.2	27.2	1	411,661	66.8	167.9
Average		40.9	2.5				6		76.3	192.0
Component B′(?)										
G9049	13.40	−12.1	259.2	348/43	30.9	259.4	2	105,310	12.3	113.5
Component C										
G9039	7.50	−25.3	277.4	346/43	15.2	276.0	2	615,645	9.4	294.5
G9041	9.00	43.5	83.9	342/53	−8.8	80.7	1	632,663	4.7	121.0
G9043	10.70	39.3	77.2	344/44	−4.7	76.5	1	597,645	9.3	122.0
G9046	13.60	−30.7	272.2	347/43	11.1	270.3	1	594,645	3.6	296.2
G9047	14.55	−3.6	289.1	342/39	26.9	294.5	1	567,587	28.0	289.0
G9048	15.30	−29.3	289.0	346/43	8.1	284.7	2	609,639	14.2	286.3
G9049	15.75	−18.1	278.1	348/43	22.4	278.7	2	587,624	13.9	296.2
G9051	18.15	−20.9	281.5	351/53	29.0	283.0	1	597,616	19.5	297.0
Average (SW)					18.9	281.0	6		−14.6	113.2
Average (NE)					−6.7	78.6	2		7.0	121.5
Average					16.1	275.2	8		−9.0	115.4
Central Greece										
Karpenissi I										
Component B										
G9057	2.64	−12.1	170.0	15/62	−27.6	194.4	1	531,570	56.0	219.7
G9059	5.11	−20.9	194.6	15/62	−10.0	213.5	1	531,590	59.0	173.0
G9060	5.22	−13.8	173.1	15/62	−25.6	197.6	1	203,633	57.5	214.6
Average		−15.9	179.0				3		59.1	203.7
Karpenissi II[a]										
Component B										
G9075	0.29	−5.5	6.9	29/30	6.0	7.0	2	486,633	47.8	191.5
G9076	0.33	−3.7	2.8	34/33	13.1	5.2	2	568,633	49.1	197.5
G9065	0.37	−2.6	348.5	34/27	16.4	350.9	1	396,571	48.4	219.2
G9066	0.52	−3.6	351.7	29/33	16.1	354.7	2	314,663	48.5	214.3
G9074	0.63	−13.1	346.8	24/32	6.9	345.4	2	569,653	42.8	219.8
G9067	0.85	−11.6	349.0	32/33	11.3	348.9	2	514,663	44.1	217.1
G9073	1.28	−1.7	9.5	24/36	7.1	11.2	2	590,638	49.2	187.1
G9069	1.97	−10.3	10.5	32/35	3.5	8.5	2	539,661	44.8	187.0
G9070	2.70	−8.7	1.1	34/33	9.5	1.3	1	487,634	46.7	200.2
G9071	2.83	−8.4	5.6	40/33	10.5	6.1	2	512,661	46.5	193.6
Average		−7.0	359.3				10		47.5	202.8
Northwestern Greece										
Varathi section										
Component B										
G9079	0.17	39.4	32.1	347/30	16.0	42.4	1	200,634	57.9	133.0
G9078	0.36	33.1	26.6	350/33	10.7	36.8	1	300,634	58.6	145.7
G9080	0.50	47.1	3.4	346/30	32.2	25.9	1	309,653	78.6	185.3
G9077	0.75	41.6	19.9	349/37	17.4	36.7	1	200,634	67.2	147.2
G9081	1.75	44.5	9.7	323/32	18.6	21.9	1	407,653	74.5	166.1
Average		41.6	19.0				5		67.8	148.8

Notes: I_i and D_i are *in situ* inclination and declination of paleomagnetic directions; I_c and D_c are corrected for structural tilt: strike/dip, strike and dip angles of bedding, strike is 90° counterclockwise of dip direction; N is the number of specimens analyzed; T_{low},T_{high} are the low and high-temperature steps of the isolated components; λ_{VGP} and ϕ_{VGP} are latitude and longitude of virtual geomagnetic pole (VGP).

[a] Depths from top of the chert section.

have been recalculated using reference poles from Besse and Courtillot (2002, 2003); and Van der Voo (1993), and are relative to stable Europe). van Hinsbergen et al. (2005a) reported similar CW rotations for a section of Plio–Pleistocene blue marls and silts exposed at the southern tip of the Koroni Peninsula (also called the Messinia Peninsula; I=−21.8°, D=190.8°, Fig. 1, locality 11).

Characteristic northwesterly declinations for Plio–Pleistocene sediments overlying the Mesozoic Pindos–Olonos Zone in central Koroni (I=32°, D=350°, N=6, k=19, α_{95}=15.6°; Fig. 1, locality 12), however, also indicate CCW rotations (van Hinsbergen et al., 2005a).

Paleomagnetic directions of Miocene andesites of the Evvia region indicate much larger (~45°) CW rotations (I=40.3°, D=50.8°, N=4, k=55, α_{95}=12.5°; Fig. 1, locality 10; Morris, 1995) confirming earlier work on similar rocks in the region by Kissel et al. (1989). In contrast, lower Oligocene Flysch units of the Gavrovo–Tripolitza Zone (I=10°, D=273.9°, Fig. 1, locality 13) exposed at Pylos on the western part of the Koroni Peninsula apparently show large-scale CCW rotations (van Hinsbergen et al., 2005a).

Morris (1995) reported pre-folding paleomagnetic directions for a middle to upper Cretaceous limestone unit of the Pindos Zone on the NE Peloponnesus, and determined that this unit had experienced mostly CW rotations averaging 36°±11° (I=30.3°, D=35.0°, N=8, k=23, α_{95}=11.8°; Fig. 1, locality 2). This rotation agrees with the overall pattern for middle and upper Cretaceous rocks of the Ionian and Sub-Pelagonian Zones, which have consistent CW rotations from southern Albania to the NE Peloponnesus (Mauritsch et al., 1995; Kondopoulou, 2000). Paleomagnetic data from Anisian–Carnian and Oxfordian limestones of the Beotia and Evvia regions presented by Morris (1995) indicate post-Jurassic CW rotations of 35°±10° and 50°±17° (I=47.9°, D=69.2°, N=11, k=22, α_{95}=9.9°; I=39.6°, D=67.4°, N=3, k=38, α_{95}=20.4°; Fig. 1, locality 3), respectively.

An even larger CW rotation (65°±14°) was reported by Pucher et al. (1974) for Middle Jurassic(?) diabase rocks from central Argolis (I=19°, D=82°, α_{95}=17°; Fig. 1, locality 4). Jurassic sedimentary rocks in the Sub-Pelagonian Zone from northern Argolis (Toarcian–Middle Jurassic; Fig. 1, locality 5; Turnell, 1988) contain a pre-folding magnetization (I=38°, D=70°, N=7, k=23, α_{95}=13°) in red to pink nodular marly limestones that indicates post-Middle Jurassic CW vertical-axis rotations of 54°±12° relative to stable Europe. Paleomagnetic directions for the Ammonitico Rosso of Middle Jurassic age exposed at Bafi (Surmont, 1989), however, indicate much larger (~130°) CCW rotations (I=28.7°, D=252.6°, α_{95}=1.8°; Fig. 1, locality 7).

Triassic rocks of the Sub-Pelagonian Zone have been sampled for paleomagnetic analysis at several localities on the Argolis Peninsula and on the Island of Hydra. Morris (1995) reports characteristic directions of magnetization from limestones of Anisian–Ladinian age exposed on the Argolis Peninsula (I=35.0°, D=82.4°, N=5, k=110, α_{95}=7.3°; Fig. 1, locality 8) indicating 37°±7° of clockwise rotation. The magnetostratigraphic analyses of Anisian–Ladinian limestones on the Island of Hydra by Muttoni et al. (1997) indicate larger (120°±25°) post-Triassic CW vertical-axis rotations (I=25.7°, D=166.0°, N=3, k=20, α_{95}=28.0°; Fig. 1, locality 9).

4. Sampled localities

Paleomagnetic directions for the middle to upper Jurassic radiolarian cherts of the continental margin unit of the Sub-Pelagonian Zone on Argolis were determined at two localities, Kandhia and Koliaky (Fig. 1). The average bedding attitude at Koliaky (strike/dip: ~N330°E/70°E) is significantly different than the bedding attitude at Kandhia (~N90°E/40°S). The outcrop at Kandhia, located in a quarry about 10 km southeast of Navplio (Fig. 1; Table 1), has red radiolarian cherts overlying the Ammonitico Rosso Formation which is in turn overlain by the Potami Breccia (0 m in Table 1 corresponds with the first chert bed above the Ammonitico Rosso Formation). Similarly, the radiolarian cherts near the village of Koliaky overlie detrital limestone and breccia beds in outcrops along the road to Palea Epidavros (Fig. 1; 0 m in Table 1 corresponds with the first chert bed above the detrital limestone). Biostratigraphic determinations by Baumgartner (1985) and Baumgartner et al. (1993) indicate that the radiolarian cherts at Kandhia are of Oxfordian age, while those at Koliaky are Bathonian to Callovian in age. A small outcrop of upper Triassic (Rhaetian; Chiari, 2001) radiolarian cherts above basalts was collected at Palea Epidavros (Fig. 1; Table 1) and the average bedding attitude at this locality is N34°E/20°E.

Paleomagnetic samples of upper Jurassic (Dogger?) to Cretaceous red radiolarian cherts of continental margin units in the Pindos–Olonos Zone (De Wever and Thiébault, 1981) on the Koroni Peninsula of the western Peloponnesus were collected in a quarry exposed along the road from Adriani to Ano Militsa (Fig. 1; Table 1). At this locality a continuous section of radiolarian chert beds is exposed dipping to the E (~N344°E/45°E). Since only the top of the unit is exposed (in stratigraphic contact with overlying cherty limestones) the depths shown in Table 1 are relative to the uppermost chert bed. De Wever and Thiébault (1981) dated the uppermost 10 m of the chert section as Turonian to Campanian in age based on the occurrence of a Campanian foraminifer (*Globotruncana* sp.) in the overlying bedded cherty limestones. However, the radiolarian assemblages in the chert beds below the limestone beds showed a poorly constrained biostratigraphic age (late Jurassic to late Cretaceous) raising questions concerning this age assignment. Since most of the chert samples with high-temperature characteristic magnetizations at Adriani were collected from the upper part of the outcrop, we assume that the cherts at this level were initially magnetized between the late Jurassic and late Cretaceous.

In continental Greece, two separate but adjacent radiolarian chert sections of continental margin units within the Pindos–Olonos Zone were sampled near the town of Karpenissi (localities I and II; Fig. 1; Table 1). The two localities are located in a tectonically complex region bound to the west by the NS-trending Pindos Thrust, and to the south by a system of EW-trending Plio–Pleistocene normal faults (Fig. 1). van Hinsbergen et al. (2006) interpreted the latter faults as part of a larger system of curved extensional Plio–Pleistocene basins that extends from the Gulf of Amvrakikos to the west, to the Gulf of Evvia to the east. Upper Jurassic chert beds at the two localities (De Wever and Cordey, 1986) have similar attitudes and the sections have similar thicknesses, although the beds at locality I dip more steeply (N15°E/62°E) than at locality II (~N30°E/30°E). Samples of Middle Jurassic radiolarian-rich marl beds of the Ionian Zone (Baumgartner et al., 1993) were also collected near Varathi (bedding attitude: ~N350°E/30°E) in the Varathi area of northwestern Greece (Fig. 1; Table 1).

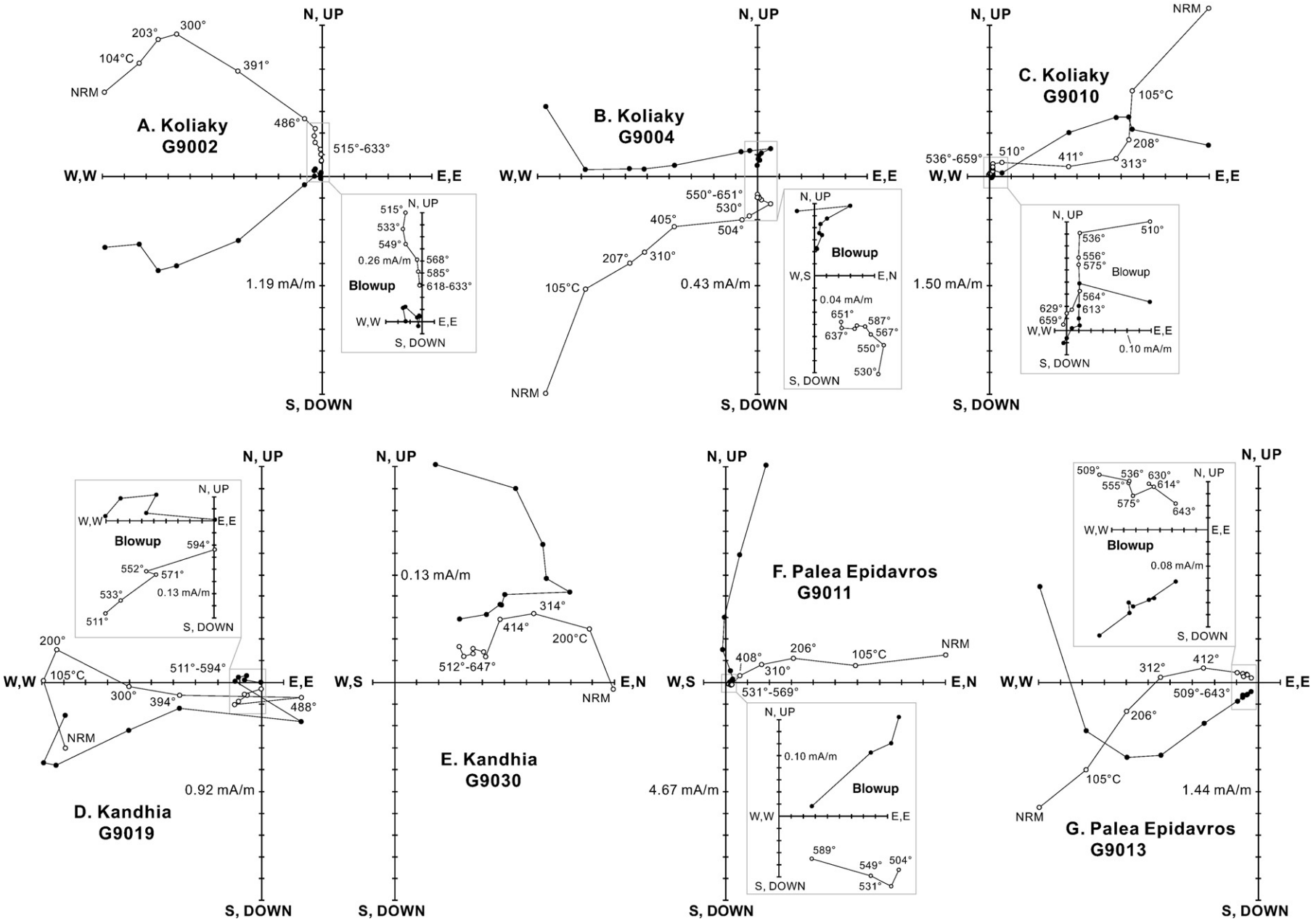

Fig. 2. Orthogonal projections (*in situ*) of thermal demagnetization vector endpoints for selected chert samples: filled circles, horizontal plane; open circles, vertical plane. A, sample G9002 from Koliaky showing components A (poor), B and negative-inclination C. B, sample G9004 from Koliaky showing a positive-inclination C component. C, sample G9010 from Koliaky showing a negative-inclination C component. D, sample G9019 from Kandhia showing components A, B and a positive-inclination C component. E, sample G9030 from Kandhia showing a reversed-polarity C component. F, sample G9011 from Palea Epidavros showing a positive-inclination C component. G, sample G9011 from Palea Epidavros showing a negative-inclination C component.

5. Methods

Since radiolarian cherts are generally too durable to be drilled in the field, oriented hand samples were collected from all sections and bedding attitudes were taken for each sample. Red cherts were selectively sampled, and zones of alteration and recrystallization were avoided. The hand samples were drilled in the laboratory with a water-cooled drill press, and 2 or more cores were drilled from most of the samples. The core samples were cut into specimens ~2.5 cm in length, and the specimens were subjected to progressive thermal demagnetization in a magnetically shielded oven to maximum temperatures of ~680 °C. Remanent magnetizations were measured using a cryogenic magnetometer, and both the oven and magnetometer are housed within a geomagnetic field-free room. Lines representing the characteristic and overprint magnetization directions were fitted to the demagnetization endpoints using a least squares method based on principal component analysis

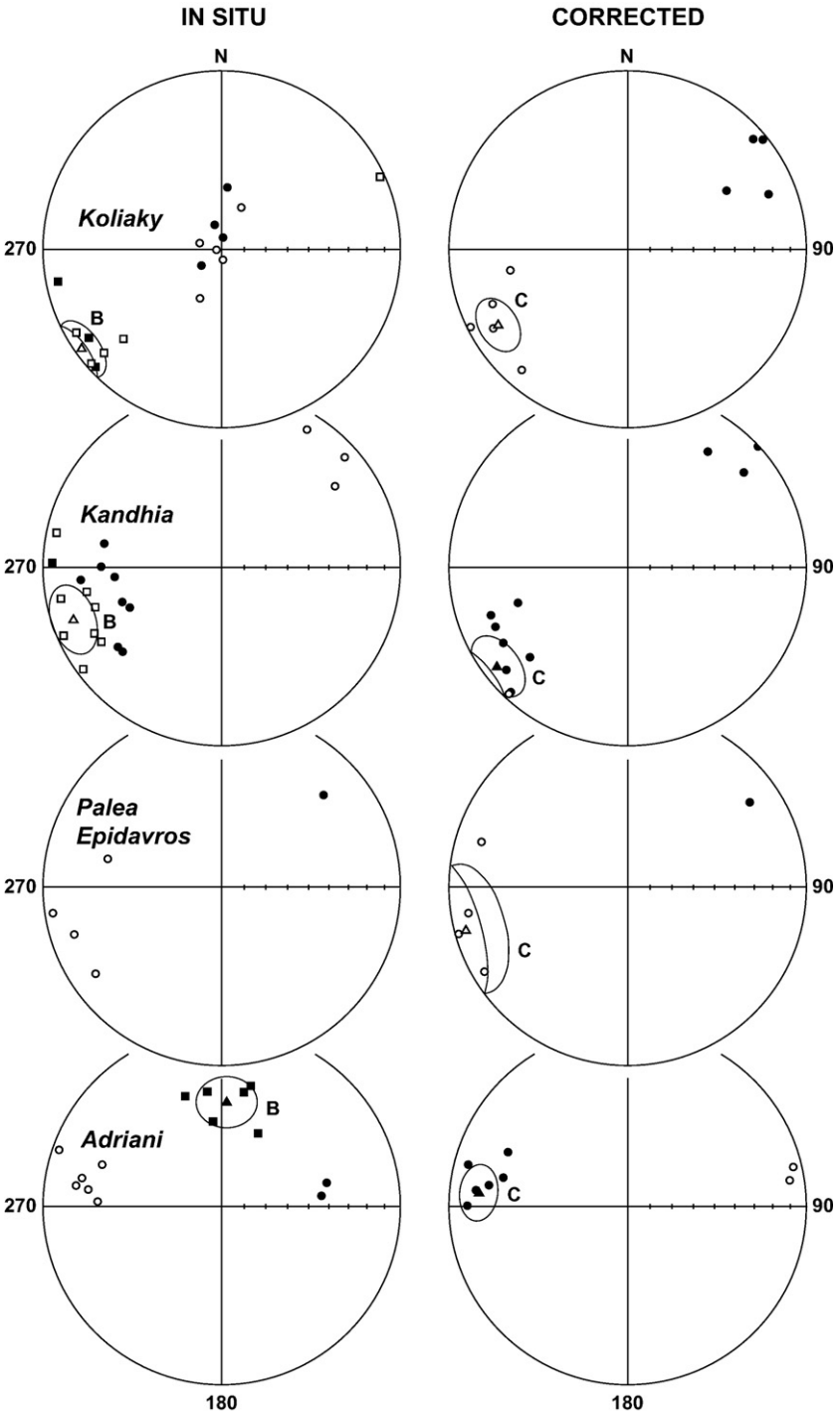

Fig. 3. Equal-area plots of sample and component mean directions (with 95% confidence limits; Table 2) for chert sections at Koliaky, Kandhia, Adriani (Koroni), and Palea Epidavros: filled (open) symbols indicate lower (upper) hemisphere points.

(Kirschvink, 1980). Components of remanent magnetization were isolated in 60 samples from radiolarian chert beds collected on the Peloponnesus and in continental Greece. Paleomagnetic directions were averaged at the sample level and the statistics of Fisher (1953) were used in analyzing the mean directions and virtual geomagnetic poles (VGPs; Table 1).

6. Results

6.1. Koliaky and Kandhia (Argolis)

Orthogonal thermal demagnetization diagrams for specimens from the Koliaky and Kandhia sections show three distinct components of magnetization (Table 1; Fig. 2A–E). The initial component (A) found in some samples was usually removed by ~300 °C and has *in situ* directions close to the localities' present-day field direction (PDF). The intermediate component (B) found in most samples was generally removed between 300 °C and 600 °C. For the samples from Koliaky it has *in situ* southwesterly declinations, and shallow inclinations; similar B directions are also reported for the samples from Kandhia (Fig. 3). Although within each locality the fold test is inconclusive, the *in situ* section-mean directions of component B clearly fail a regional-scale fold test.

A third characteristic component (C) was isolated between 400 °C and 670 °C in specimens from both sections (Table 1;

Table 2
Mean paleomagnetic directions, paleolatitudes, and poles for chert sections in Greece

Section	I (°)	D (°)	Strike/dip (°/°)	N/N_o	R	k	α_{95} (°)	λ_{PAL} (°)	λ_{VGP} (°N)	ϕ_{VGP} (°E)
Component C										
Argolis Peninsula										
Koliaky (37.639°N, 23.159°E)										
All	−15.9	239.6	334/72	9/10	8.6673	24	10.7	8±6	28.9	126.0
NE	15.3	56.8		4/10	3.8681	23	19.7		30.9	128.3
SW	−16.3	241.9		5/10	4.8073	21	17.2		27.2	124.2
Kandhia (37.530°N, 22.984°E)										
All	8.6	232.9	88/41	11/13	10.3133	15	12.4	4±7	25.8	141.4
NE	13.3	44.4		3/13	2.9397	33	21.8		39.4	139.0
SW	16.7	235.7		8/13	7.7030	24	11.6		20.6	142.2
Average										
Unc	59.5	253.5		20/23	15.9171	5	17.0			
Cor	2.6	55.8		20/23	18.5201	13	9.5	1±5	27.4	134.5
Palea Epidavros (37.639°N, 23.159°E)										
	−6.6	255.4	34/20	5/8	4.6747	12	22.7	3±12	13.6	119.5
Koroni Peninsula										
Adriani (36.867°N, 21.893°E)										
All	16.1	275.2	344/45	8/15	7.7546	29	10.6	8±4	−9.4	115.4
E	−6.7	78.6		2/15	1.9974	–	–		7.0	121.5
W	18.9	281.0		6/15	5.8978	49	9.7		−14.6	113.2
Component B										
Argolis Peninsula										
Koliaky (37.639°N, 23.159°E)										
	−4.0	234.7		9/10	8.6653	24	10.7	2±5	28.6	134.8
Kandhia (37.639°N, 23.159°E)										
	−12.7	250.5		10/13	9.4081	15	12.8	6±7	19.3	119.9
Koroni Peninsula										
Adriani (36.867°N, 21.893°E)										
	40.9	2.5		6/15	5.8247	29	12.8	23±11	1.8	97.3
Central Greece										
Karpenissi I (38.927°N, 21.754°E)										
	−15.9	179.0		3/10	2.9437	36	21.0	8±12	59.1	203.7
Karpenissi II (38.949°N, 21.757°E)										
	−7.0	359.3		10/13	9.8617	65	6.0	3±7	47.5	202.8
Average										
Unc	−1.8	359.2		13/23	12.6259	32	7.4	1±3	50.2	203.0
Cor	12.8	4.1		13/23	12.6759	37	6.9	6±2	57.3	194.2
Northwestern Greece										
Varathi (39.362°N, 20.538°E)										
	41.6	19.0		5/5	4.9360	63	9.7	24±8	67.8	148.8

Notes: I and D are inclination and declination of paleomagnetic directions corrected (cor) for structural tilt (unc, uncorrected; component B *in situ*); strike/dip of bedding (dip 90° clockwise of strike); N/N_o is the number of sample directions averaged/samples collected; R is the vector sum of N unit vectors; k is the concentration parameter (Fisher, 1953); α_{95} is the radius of the 95% confidence circle; λ_{PAL} is paleolatitude with 95% confidence limits; λ_{VGP} and ϕ_{VGP} are latitude and longitude of the virtual geomagnetic pole (VGP).

Fig. 2A–E). At Koliaky, where beds are steeply dipping, component C has *in situ* directions with steep antipodal positive and negative inclinations (Fig. 2A–C). After correcting for bedding tilt the sample directions move to NE–SW declinations and shallow inclinations (Fig. 3). The average direction of the NE group is $I=15.3°$, $D=56.8°$, $N=4$, $k=23$, $\alpha_{95}=19.7°$, and the average direction of the SW group is $I=-16.3°$, $D=241.9°$, $N=5$, $k=21$, $\alpha_{95}=17.2°$ (Table 2). After inversion of the westerly group ($I=16.3°$, $D=61.9°$) the two directions are statistically indistinguishable at the 95% confidence level (McFadden and Lowes, 1981), and are 5.0° (γ_c) apart passing the reversal test of McFadden and McElhinny (1990).

At Kandhia, where the bedding attitude is shallower, component C has *in situ* NE–SW declinations and low inclinations (Table 1; Fig. 2D–E), and the SW group has declinations similar to component B (Fig. 3). After correction for bedding tilt the inclination of the SW group becomes shallower, and the NE group moves to shallow positive inclinations. The average direction of the NE group is $I=13.3°$, $D=44.4°$, $N=3$, $k=33$, $\alpha_{95}=21.8°$, and the average direction of the SW group is

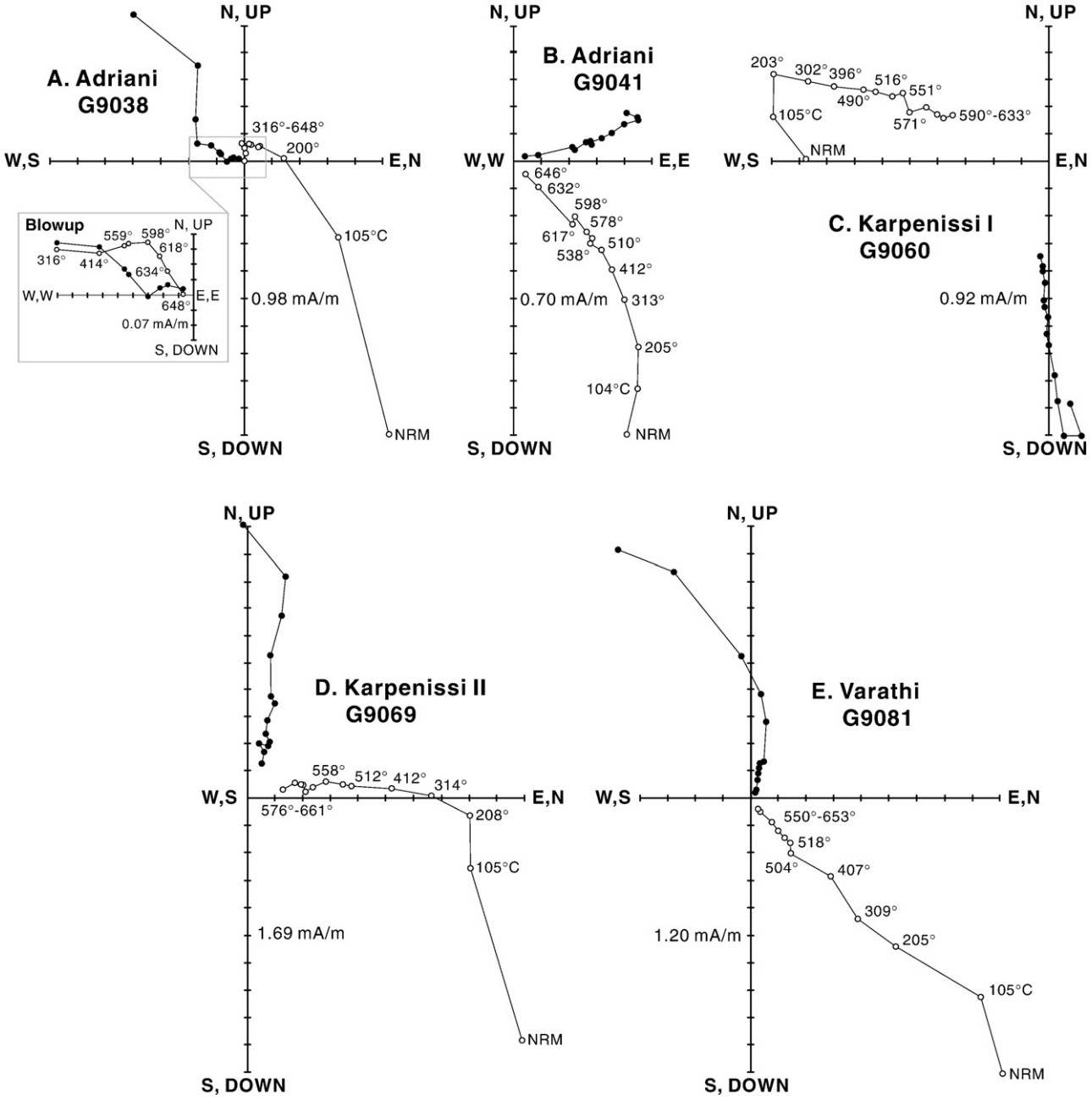

Fig. 4. Orthogonal projections (*in situ*) of thermal demagnetization vector endpoints for selected chert samples: filled circles, horizontal plane; open circles, vertical plane. A, sample G9038 from Adriani (Koroni) showing components A, B and a negative-inclination C. B, sample G9041 from Adriani (Koroni) with a positive-inclination C component. C, sample G9060 from Karpenissi (locality I) showing component A and a southerly component B. D, sample G9069 from Karpenissi (locality II) showing component A and a northerly component B. E, sample G9081 from Varathi showing component A and a northerly component B.

I=16.7°, D=235.7°, N=8, k=24, α_{95}=11.6°. After inversion of the SW group (I=−16.7°, D=55.7°), the average directions of the two groups are statistically distinct at the 95% confidence level (McFadden and Lowes, 1981), and γ_c=32° indicating an indeterminate reversal test (McFadden and McElhinny, 1990). Although the separation in declination indicates that both polarities of the field have most likely been recorded, the non-antipodal directions are probably due to incomplete removal of the similar B overprint magnetization. However, the C directions are better grouped after bedding correction (k_1=5 versus k_2=13; Table 2) indicating that the C magnetization likely predates deformation. The corrected overall mean for the C component for the two Jurassic sections of radiolarian chert on the Argolis Peninsula is I=2.6°, D=55.8°, α_{95}=9.5°, with a paleolatitude of 1°±5° N or S.

6.2. Palea Epidavros (Argolis)

For the Triassic radiolarian cherts at Palea Epidavros, vector endpoints of the thermal demagnetization diagrams show two components of magnetization (Table 1; Fig. 2F–G). After removal of the A component by 200° to 300 °C, the characteristic C component was isolated between 400 °C and 660 °C. Component C has mostly southwesterly *in situ* directions and shallow inclinations (Fig. 3). Only one sample shows an antipodal easterly direction and positive inclination. Thus, component C could be interpreted as a primary magnetization, although a quantitative reversal test for the C component is inconclusive (McFadden and McElhinny, 1990). Assuming that component C is primary, the corrected mean direction is I=−6.6°, D=255.4°, N=5, k=12, α_{95}=22.7°, corresponding to a paleolatitude of 3°±12° (Table 2).

6.3. Adriani (Koroni)

Thermal demagnetization diagrams for chert samples from Adriani also show three components of magnetization (Table 1; Fig. 4A–B). The initial PDF component (A) was removed in almost all samples by about 300 °C. The intermediate component (B) is generally removed between 300 °C and 600 °C and has *in situ* northerly declinations and intermediate positive inclinations (Fig. 3). The third characteristic component (C) was isolated between ~500 °C and 630 °C. Component C has both westwards and eastwards *in situ* declinations, and after correction shallow inclinations (Fig. 3). The average direction of the easterly group is I=−6.7°, D=78.6°, N=2, and the average direction of the westerly group is I=18.9°, D=281.0°, N=6, k=49, α_{95}=9.7° (Table 2). Again, although two polarities apparently have been recorded a quantitative reversal test is inconclusive. After inversion of the easterly group the overall mean direction for the C component is I=16.1°, D=275.2°, N=8, k=29, α_{95}=10.6°, indicating a paleolatitude of 8°±4° (Table 2).

6.4. Karpenissi (localities I and II)

Both radiolarian chert sections studied at Karpenissi show two components of remanent magnetization (Fig. 4C–D; Fig. 5). The viscous PDF component (A) was removed in some of the samples by about 400 °C, and a second component was removed between 200 °C and 660 °C. At locality I the characteristic component has *in situ* southerly declinations and shallow negative inclinations I=−15.9°, D=179.0°, N=3, k=36, α_{95}=21.0° (Table 2; Fig. 5), and at locality II it has *in situ* northerly declinations and shallow negative inclinations I=−7.0°, D=359.3°, N=10, k=65, α_{95}=6.0°. Although the reversal test for these two directions is indeterminate, the characteristic component appears to have been acquired during at least one polarity reversal. The lack of any polarity structure in either of these sections, particularly locality II, however, indicates that this magnetization is most likely secondary (B). A possible fold test between the two localities is also inconclusive (k_1=32 versus k_2=37; Table 2).

6.5. Varathi

The thermal demagnetization diagrams for specimens from Varathi also show two components (Figs. 4E and 5). The

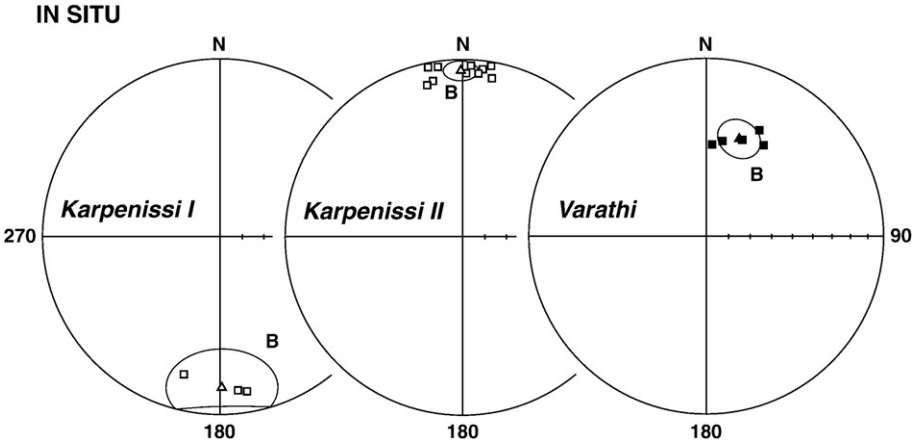

Fig. 5. Equal-area plots of chert sample and mean (with 95% confidence limits) directions for section localities I and II at Karpenissi and at Varathi: filled (open) symbols indicate lower (upper) hemisphere points.

characteristic component was isolated between 200 °C and 660 °C (Table 2) has mostly northerly *in situ* directions, and intermediate normal inclinations I=41.6°, D=19.0° (Fig. 5). Again, the lack of both polarities and the similarity to the PDF direction indicate that this magnetization is secondary.

7. Discussion

7.1. Primary magnetization and vertical-axis rotations for radiolarian cherts from the Peloponnesus

7.1.1. Koliaky and Kandhia (Argolis)

The similarity of mean *in situ* B directions for the chert sections at Kandhia and Koliaky (Table 2), and the *in situ* directions of the magnetic overprint reported by Muttoni et al. (1997) in Triassic limestones on the island Hydra (I=−20°, D=225°), suggests that component B is a magnetic overprint acquired during or after a regional-scale tectonic event. Assuming that the sections have undergone little structural deformation since overprinting, the easterly directions indicate a total post-overprint CW vertical-axis rotation of ~60° for both Argolis and Hydra. The average inclination of the magnetic overprint for the Argolis samples, however, is ~12° shallower than that from Hydra. Since the post-Miocene rotation for the Pelagonian Zone in the nearby region of Beotia is ~45° CW (Morris, 1995), we suggest that component B was acquired prior to the Miocene, probably during or after the Eocene "Meso-Hellenic" phase.

Component C for both the Koliaky and Kandhia chert sections passes a regional fold test, shows both normal and reverse polarities, and has high unblocking temperatures. We interpret component C as the primary magnetization acquired during or soon after the deposition of the radiolarian-rich sediment layer precursors of the chert beds. Average C component inclinations for the red cherts of Argolis (9° to 16°; Table 2) are in agreement with the mean inclination for the Middle Jurassic diabase (19°) reported by Pucher et al. (1974).

The average direction of component C from both Koliaky and Kandhia indicates a post-Jurassic CW vertical-axis rotation of ~40° for the continental margin units of Argolis relative to stable Europe (Table 3). Although the hemisphere of origin (N or S) and thus paleomagnetic polarity are unknown, these vertical-axis rotations could be either CW or CCW. They are, however, similar to those calculated for Middle Jurassic diabases (~65° CW) on central Argolis (Pucher et al., 1974), the limestones of Anisian–Ladinian age (~35° CW) exposed on Argolis (Morris, 1995), and directions for the Anisic to Oxfordian limestones (~50° CW) of the Beotia–Evvia region (Morris, 1995). Morris (1995) suggests that the post-Jurassic CW vertical-axis rotation of the Sub-Pelagonian Zone occurred

Table 3
Paleomagnetic poles for Greece, Europe, and, Africa

Locality (ref pole)	λ_{Pole} (°N)	ϕ_{Pole} (°E)	N	R	K	α_{95} (°)	d (°)	r (°)
Argolis Peninsula								
Koliaky (E: 160 Ma)	28.9	125.5	9	8.7795	36	8.7	19±8	43±8
Koliaky (A: 160 Ma)	28.9	125.5	9	8.7795	36	8.7	6±8	90±8
Kandhia (E: 160 Ma)	25.5	141.4	11	10.6471	28	8.7	32±8	36±8
Kandhia (A: 160 Ma)	25.5	141.4	11	10.6471	28	8.7	19±8	83±8
Average (E: 160 Ma)	27.2	134.3	20	19.2719	26	6.5	26±3	40±7
Average (A: 160 Ma)	27.2	134.3	20	19.2719	26	6.5	13±6	86±6
Palea Epidavros (E: 210 Ma)	20.7	117.5	5	4.7869	19	18.1	9±18	33±18
Palea Epidavros (A: 210 Ma)	20.7	117.5	5	4.7869	19	18.1	10±15	80±15
Koroni Peninsula								
Adriani (E: 90 Ma)	−9.4	115.4	8	7.8084	37	9.3	37±8	95±9
Adriani (E: 150 Ma)	−9.4	115.4	8	7.8084	37	9.3	34±9	84±9
Adriani (A: 90 Ma)	−9.4	115.4	8	7.8084	37	9.3	28±8	113±8
Adriani (A: 150 Ma)	−9.4	115.4	8	7.8084	37	9.3	22±9	128±9
Europe (E)								
Cretaceous (90 Ma)[a]	82	202	13	n.a.	65	5		
Late Jurassic (150 Ma)[a]	75	160	10	n.a.	54	7		
M/L Jurassic (160 Ma)[a]	73	144	15	n.a.	60	5		
Triassic (216–232 Ma)[b]	52	133	5	n.a.	29	14		
Africa (A)								
Cretaceous (90 Ma)[a]	67	249	13	n.a.	73	5		
Late Jurassic (150 Ma)[a]	53	261	10	n.a.	62	6		
M/L Jurassic (160 Ma)[a]	55	260	15	n.a.	57	5		
Triassic (196–215 Ma)[b]	70	230	4	n.a.	163	7		

Note: λ_{Pole} and ϕ_{Pole} are latitude and longitude of paleomagnetic poles; N, R, K, and α_{95} as in Table 1; d and r are the poleward displacement and clockwise rotation of the sampling locality relative to the reference poles (ref pole) using the method of Beck (1980) as modified by Demarest (1983); n.a. indicates not available.

[a] Besse and Courtillot (2002, 2003; Table 4).

[b] Van der Voo (1993; Tables 5.1 and 5.3).

in a uniform rotational domain that extended from Argolis to Beotia and Evvia, and that the total observed rotation can be separated into a ~20° CW phase that occurred in pre-Middle Miocene time and a subsequent ~45° CW Neogene phase. The similarity between the directions of component B (*in situ*) and C (corrected for bedding), however, suggests that no significant vertical-axis rotations have occurred between the deposition of the chert beds (Middle Jurassic) and the time of magnetic overprinting (possibly Eocene).

As discussed earlier, paleomagnetic directions of shallow-water limestones exposed on Hydra indicate large (~120°) CW vertical-axis rotations relative to stable Europe since Triassic time (Muttoni et al., 1997). These rotations are much larger than those reported from other coeval limestones on Argolis (Morris, 1995), and from those determined in this study for the Middle Jurassic radiolarian cherts of Argolis (~40° CW; Table 2). It is possible, however, that the similarity in directions for component B of the radiolarian cherts on Argolis and Hydra (Muttoni et al., 1997) indicate that any differential rotation between the two occurred prior to the time of magnetic overprinting (possibly Eocene).

7.1.2. Palea Epidavros (Argolis)

At Palea Epidavros, most of the samples show westerly directions and shallow inclinations ($I=-6.6$, $D=255.4$) and only one sample shows the opposite polarity. Moreover, the within-section fold test for the high-temperature component C is inconclusive. Although not as conclusive as the evidence for the Jurassic chert sections at Koliaky and Kandhia, we tentatively interpret component C as the primary magnetization acquired during the Triassic and also indicating a similar post-Triassic CW vertical-axis rotation (~33°) of the continental margin of Argolis relative to stable Europe (Table 3).

7.1.3. Adriani (Koroni)

The results of our paleomagnetic analyses of the Mesozoic units of the upper Jurassic to upper Cretaceous radiolarian cherts exposed at Adriani indicate that component B has northerly declinations and medium positive *in situ* inclinations ($I=40.9°$, $D=2.5°$). The comparison between the directions of component B and the declinations of the characteristic magnetization of the Plio–Pleistocene sediments ($I=-32°$, $D=160°$; locality 12) overlying Mesozoic Pindos–Olonos units a few kilometers northeast of Adriani (van Hinsbergen et al., 2005a) suggest that component B was acquired after the Plio–Pleistocene.

After correction for bedding, component C shows antipodal groups and shallow inclinations (average $I=16.1°$, $D=275.2°$) and is tentatively interpreted as a primary magnetization (Fig. 3). The declination of component C also suggests a total CW or CCW vertical-axis rotation of ~95° or ~84° for Adriani, respectively, relative to stable Europe in the upper Cretaceous (Table 3).

The characteristic directions of magnetization found at Adriani are similar to those reported by van Hinsbergen et al. (2005a) for the lower Oligocene Flysch units of the Gavrovo–Tripolitza Zone ($I=10°$, $D=273.9°$ and $I=-23.8°$, $D=89.8°$) exposed at two separate sites near Pylos in the southwestern part of the Koroni Peninsula. The remanent magnetizations for the lower Oligocene Flysch units of the Gavrovo–Tripolitza Zone, however, are either local or unreliable (van Hinsbergen et al., 2005a). Moreover, CCW rotations are not supported by the local directions of fold axes and thrusts that follow the regional NNW–SSE trend, and the shallow inclinations recorded at Pylos are not compatible with the position of the Oligocene Flysch Unit of the Gavrovo–Tripolitza Zone during the lower Oligocene. A CCW sense of rotation for component C at Adriani would contradict the majority of CW rotations observed for coeval or younger rocks on the Peloponnesus, and indicates that this section of radiolarian cherts was also rotated CW since Cretaceous time. Further paleomagnetic investigation of the Koroni peninsula is necessary, however, to better understand the tectonic rotations in the westernmost sector of the Peloponnesus.

7.2. Magnetic overprint of radiolarian cherts in continental Greece

At Karpenissi, the characteristic magnetization found at locality II has northerly declinations and shallow negative inclinations ($I=-7.0$, $D=359.3$), while at locality II the paleomagnetic directions are nearly antipodal ($I=-15.9$, $D=179.0$). This result was unexpected since the two localities are close to one another, and have similar bedding attitudes and section thicknesses. If we interpret this magnetization as an overprint, two possible explanations can be envisaged to explain the different directions recorded at the two localities: (1) tectonic deformation has affected the region after the acquisition of the magnetic overprint, and (2) the two localities have acquired the magnetic overprint at different times recording both polarities of the magnetic field characterized by shallow inclinations and northerly declinations ($I=12.8°$, $D=4.1°$).

At Varathi we interpret component B as a magnetic overprint. It is worth noting that the average direction of this component ($I=41.6°$, $D=19.0°$) shows a strong similarity with component B found at Adriani ($I=40.9°$, $D=2.5°$; Table 2).

7.3. Paleolatitudes of Mesozoic radiolarian cherts in Peloponnesus

The paleolatitudes calculated for Kandhia and Koliaky (middle to upper Jurassic chert) tend to be quite low (1° to 8°; Table 2; Fig. 6), and our paleomagnetic data do not allow us to determine whether Argolis was in the northern or southern hemisphere during the Middle Jurassic. However, since the magnetostratigraphic correlations proposed by Muttoni et al. (1997) indicate that Hydra was in the northern hemisphere during middle Triassic, we suggest that a similar conclusion can be also extended to the Jurassic radiolarian chert sections sampled on Argolis. The characteristic magnetization for the upper Jurassic to upper Cretaceous cherts exposed at Adriani (Koroni) has also been tentatively interpreted as a primary magnetization, which gives a paleolatitude of 8°±4° (Table 2; Fig. 6). In addition, the paleolatitude for the Triassic cherts at Palea Epidavros is near equatorial (3°±12°; Table 2; Fig. 6) although the interpretation of this component as primary is also tentative.

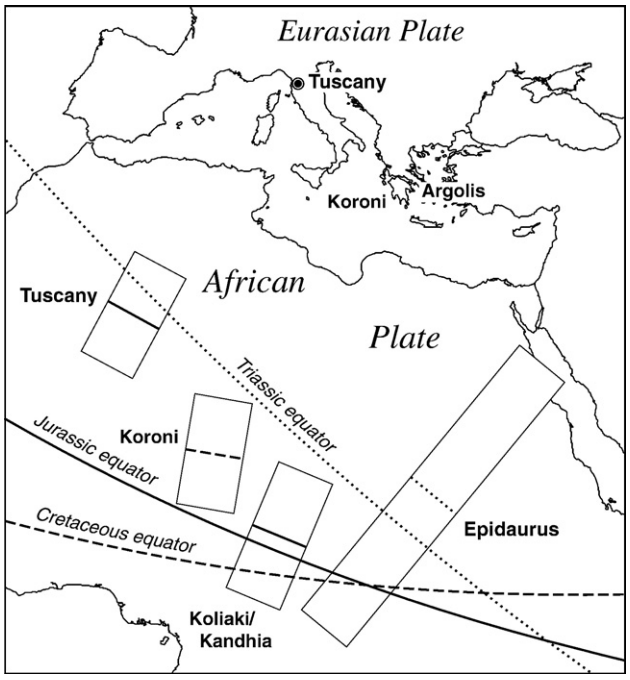

Fig. 6. Paleolatitudes for Mesozoic radiolarian cherts from Greece (this study) and Tuscany (Aiello and Hagstrum, 2001) plotted on a present-day map of the Mediterranean and North African region. Box for each locality represents the 95% error limits, and the estimated paleolatitude (Table 2) is coded to the equator corresponding to the coeval paleomagnetic reference pole (Table 3); paleolongitudes are undefined. The Koliaky, Kandhia, and Palea Epidavros sections are located on the Argolis Peninsula (Fig. 1).

The inclinations of component (C) for at Koliaky, Kandhia, and possibly Koroni, indicate that deposition of the Mesozoic cherts in the Sub-Pelagonian and Pindos–Olonos Zones of the Peloponnesus occurred at peri-equatorial latitudes (Table 2; Fig. 6). These data are similar to those obtained for Mesozoic radiolarian cherts in Italy (11°±5° N; Aiello and Hagstrum, 2001), the Mino Terrane of central Japan (1°±3° N or S; Shibuya and Sasajima, 1986), and along the western margin of North America in California (Hagstrum and Murchey, 1993; Hagstrum et al., 1996) and western Mexico (0°–2° N or S; Hagstrum and Sedlock, 1992). Peri-equatorial paleolatitudes for Jurassic radiolarian cherts of the Peloponnesus further support the hypothesis that they were deposited within zones of equatorial upwelling, high biologic productivity, and preservation of radiolarian tests on the seafloor (Aiello and Hagstrum, 2001; Muttoni et al., 2005).

An alternative interpretation for the low inclinations found in Greek radiolarian cherts, as well as in the other sections of Mesozoic cherts, is that they are lowered by diagenetic compaction and flattening of the magnetic fabric. Previous sedimentologic and petrographic studies have shown, however, that early diagenesis producing semi-lithified sediments was common in Jurassic cherts of the Northern Apennines as indicated by deformation of beds during intraformational slumping, by rotation of coherent beds, and by plastic deformation of bedding around detrital clasts and boulders (Aiello, 1997). The paleomagnetically-important iron oxides in radiolarian-rich sediments (hematite and magnetite) are derived mainly from continental sources, and after deposition the first ferric iron to precipitate from a saturated solution is either hematite or goethite (an iron hydroxide) that quickly dehydrates to hematite (Blatt, 1992). During precipitation and growth, the authigenic magnetic minerals acquire a stable remanent magnetization aligned with the geomagnetic field (Channell et al., 1982) that would not be subjected to significant shallowing during subsequent burial and compaction due to the early diagenesis of the radiolarian cherts.

8. Conclusions

Thermal demagnetization analyses of 60 samples from Mesozoic radiolarian cherts of continental margin units within the Pelagonian Zone of Argolis (Peloponnesus; Kandhia and Koliaky on the Argolis Peninsula), the Pindos–Olonos Zone at Adriani (Koroni Peninsula), near Karpenissi (central Greece), and the Ionian Zone at Varathi (northwestern Greece), indicate that the studied sections carry up to three components of remanent magnetization.

The moderate unblocking temperature B component is a post-depositional overprint, and at Koliaky and Kandhia has an *in situ* direction similar to that for remagnetized Triassic limestones on Hydra (Muttoni et al., 1997). Component B, therefore, was probably acquired during or after the latest regional-scale tectonic event, and, assuming little structural deformation since overprinting, indicates a CW vertical-axis rotation of ~60° for both Argolis and Hydra. The similarity of these CW rotations with those for Miocene units of the Pelagonian Zone (~51° CW; Morris, 1995) indicates that component B was acquired prior to Miocene time, possibly during or after the Eocene "Meso-Hellenic" orogenetic phase. Conversely, at Adriani and Varathi component B is probably of a more recent age (Pleistocene). At Karpenissi, a clear interpretation of component B is not possible based on the available data.

At Koliaky and Kandhia the high-temperature C component is interpreted as the primary magnetization, and mean directions indicate post-Jurassic CW vertical-axis rotations of ~40° relative to stable Europe (Table 3). A high-temperature magnetization was also found at Adriani, and possibly indicates a post-upper Cretaceous CW vertical-axis rotation of ~95° relative to stable Europe (Table 3).

Paleolatitudes calculated for the Mesozoic cherts at Koliaky, Kandhia, and Koroni are peri-equatorial (Table 2; Fig. 6), and agree with those for other Mesozoic rocks of Argolis and the Pelagonian Zone of Greece (e.g., Turnell, 1988; Morris, 1995). Low paleolatitudes have also been determined for coeval radiolarian cherts of the Italian Alps and Apennines (Aiello and Hagstrum, 2001; Muttoni et al., 2005) and for Mesozoic cherts in central Japan (1°±3° N or S; Shibuya and Sasajima, 1986), and along the western margin of North America (0°–2° N or S; e.g. Hagstrum et al., 1996). Our new data from the Peloponnesus support the hypothesis that radiolarian sedimentation in Mesozoic Tethys occurred along peri-equatorial belts of upwelling and high biological productivity.

Acknowledgments

The authors are most grateful to Adonis Photiades, Nicolas Carras and Kate Paddock for their help with the fieldwork in Greece. D. van Hinsbergen and G. Muttoni also provided helpful and constructive reviews.

References

Abbate, E., Bortolotti, V., Conti, M., Marcucci, M., Principi, G., Passerini, P., Treves, B., 1986. Apennines and Alps ophiolites and the evolution of the Western Tethys. Memorie della Società Geologica Italiana 31, 23–44.

Aiello I.W., 1997, Le rocce biogeniche silicee pelagiche della Tetide Occidentale (Giurassico): PhD Dissertation, University of Florence and Parma, Italy.

Aiello, I.W., Hagstrum, J.T., 2001. Paleomagnetism and paleogeography of Jurassic radiolarian cherts from the Northern Apennines of Italy. Geological Society of America Bulletin 113 (4), 469–481.

Aubouin, J., 1958. Essai sur l'evolution paleogeographique et le developement tecto-orogenique d'un systeme geosynclinal: Le secteur grec des Dinarides (Hellenides). Bulletin de la Societe Geologique de France 6 (8), 731–750.

Aubouin, J., Bonneau, M., Celet, P., Charvet, J., Ciement, B., Degardin, J.M., Dercourt, J., Ferrière, J., Fleury, J.J., Guernet, C., Maillot, H., Mania, J.H., Mansy, J.L., Terry, J., Thiébault, P., Tsofilias, P., Verrieux, J.J., 1970. Contribution à la géologié des Hellénides: Le Gavrovo, Le Pinde et la zone ophiolitique Subpélagonienne. Annales de la Societe Geologique du Nord 90 (4), 277–306.

Avramidis, P., Zelilidis, A., Vakalas, I., Kontopoulos, N., 2002. Interactions between tectonic activity and eustatic sea-level changes in the Pindos and Mesohellenic basins, NW Greece. Journal of Petroleum Geology 25, 53–82.

Barrett, T.J., 1982. Stratigraphy and sedimentology of Jurassic bedded chert overlying ophiolites in the North Apennine, Italy. Sedimentology 29, 353–373.

Baumgartner, P.O., 1985. Jurassic sedimentary evolution and nappe emplacement in the Argolis Peninsula (Peloponnesus, Greece). Denkschriften der Schweizerischen Naturforschenden Gesellschaft 99, 1–111.

Baumgartner, P.O., 1987. Age and genesis of Tethyan Jurassic radiolarites. Eclogae Geologicae Helveticae 90, 831–879.

Baumgartner, T.R., Danelian, T., Dumitrica, P., Gorican, S., Jud, R., O'Dogherty, L., Carter, B., Conti, M., De Wever, P., Kito, N., Marcucci, M., Matsuoka, A., Murchey, B., Urquart, E., 1993. Middle Jurassic–Early Cretaceous radiolarian biochronology of Tethys: implications for the age of radiolarites in the Hellenides (Greece). Bulletin of the Geological Society of Greece 28, 13–23.

Baumgartner, P.O., Bartolini, A.C., Carter, E.S., Conti, M., Cortese, G., Danelian, T., DeWever, P., 1995. Middle Jurassic to Early Cretaceous radiolarian biochronology of Tethys based on unitary associations. In: Baumgartner, P.O. (Ed.), Middle Jurassic to Lower Cretaceous Radiolaria of Tethys, Occurrences, Systematics, Biochronology. Mémoir Géologié (Lausanne), vol. 23, pp. 1013–1048.

Beck Jr., M.E., 1980. Paleomagnetic record of plate-margin processes along the western edge of North America. Journal of Geophysical Research 85, 7115–7131.

Besse, J., Courtillot, V., 2002. Apparent and true polar wander and the geometry of the geomagnetic field over the last 200 Myr. Journal of Geophysical Research 107 (2300). doi:10.1029/2000JB000050.

Besse, J., Courtillot, V., 2003. Correction to "Apparent and true polar wander and the geometry of the geomagnetic field over the last 200 Myr". Journal of Geophysical Research 108 (2469). doi:10.1029/2003JB002684.

Blatt, H., 1992. Sedimentary Petrology. W.H. Freeman and Company, New York. 514 pp.

Bortolotti, V., Carras, N., Chiari, M., Fazzuoli, M., Marcucci, M., Photiades, A., Principi, G., 2002. New geological observations and biostratigraphic data on the Argolis Peninsula: paleogeographic and geodynamic implications. Ofioliti 27, 43–46.

Bortolotti, V., Carras, N., Chiari, M., Fazzuoli, M., Marcucci, M., Photiades, A., Principi, G., 2003. The Argolis Peninsula in the palaeogeographic and geodynamic frame of the Hellenides. Ofioliti 28, 79–94.

Bosellini, A., Winterer, E.L., 1975. Pelagic limestones and radiolarites of the Tethyan Mesozoic: a genetic model. Geology 3, 279–282.

Channell, J.E.T., 1992. Paleomagnetic data from Umbria (Italy): implications for the rotation of Adria and Mesozoic apparent polar wander path. Tectonophysics 216, 365–378.

Channell, J.E.T., 1996. Paleomagnetism and paleogeography of Adria. In: Morris, A., Tarling, D.H. (Eds.), Paleomagnetism and Tectonics of the Mediterranean Region. Geologic Society Special Publication, 105, pp. 119–132.

Channell, J.E.T., Kozur, H.W., 1997. How many oceans? Meliata, Vardar, and Pindos oceans in Mesozoic Alpine paleogeography. Geology 25 (2), 183–186.

Channell, J.E.T., Freeman, R., Heller, F., Lowrie, W., 1982. Timing of diagenetic haematite growth in red pelagic limestones from Gubbio (Italy). Earth and Planetary Science Letters 58, 189–201.

Channell, J.E.T., Brandner, R., Spieler, A., Stoner, J.S., 1992. Paleomagnetism and Paleogeography of the Northern Calcareous Alps (Austria). Tectonics 11 (4), 792–810.

Chiari M., 2001, Biostratigrafia a Radiolari del Giurassico Medio — Cretaceo Inferiore nella Tetide Occidentale. PhD, University of Parma, Italy.

Demarest, H.H.J., 1983. Error analysis for the determination of tectonic rotation from paleomagnetic data. Journal of Geophysical Research 88, 4321–4328.

De Wever, P., Cordey, F., 1986. Datation par les radiolaires de la Formation des Radiolarites s.s. de la serie du Pinde-Olonos (Grece); Bajocien(?)-Tithonique. Radiolarian dating of the Radiolarite Formation of the Pindus-Olonos series, Greece; Bajocian(?)-Tithonian. Marine Micropaleontology 11 (1–3), 113–127.

De Wever, P., Thiébault, F., 1981. Les radiolaires d'age Jurassique superieur a Cretace superieur dans les radiolarites du Pinde-Olonos (Presqu'ile de Koroni; Peloponnese meridional, Grece). Radiolaria of Upper Jurassic to Upper Cretaceous age in the radiolarites of Pindus–Olonos, Koroni Peninsula, southern Peloponnesus, Greece. Geobios 14 (5), 577–609.

Duermeijer, C.E., Nyst, M., Meijer, P.T., Langereis, C.G., Spakman, W., 2000. Neogene evolution of the Aegean Arc; paleomagnetic and geodetic evidence for a rapid and young rotation phase. Earth and Planetary Science Letters 176 (3–4), 509–525.

Feinberg, H., Edel, B., Kondopoulou, D., Michard, A., 1996. Implications of ophiolite paleomagnetism for the interpretation of the geodynamics of Northern Greece. In: Morris, A., Tarling, D.H. (Eds.), Paleomagnetism and Tectonics of the Mediterranean Region. Geologic Society Special Publication, 105, pp. 289–298.

Fisher, R.A., 1953. Dispersion on a sphere. Royal Society of London Proceedings 217 (ser. A), 295–305.

Fleury, J.J., 1980. Les zones de Gavrovo–Tripolitza et du Pinde–Olonos (Grèce continentale et Péloponnèse du Nord). Evolution d'une plate-forme et d'un bassin dans leur cadre alpin. Societe Geologique du Nord Mémoire 4, 1–473.

Garrison, R.E., 1974. Radiolarian cherts, pelagic limestones and igneous rocks in eugeosynclinal assemblages. In: Hsü, K.J., Jenkins, H.C. (Eds.), Pelagic Sediments on Land and Under the Sea. Spec. Publ. Int. Assoc. Sedimentol., vol. 1. Blackwell Scientific Publications, pp. 367–399.

Hagstrum, J.T., Sedlock, R.L., 1992. Paleomagnetism of Mesozoic red chert from Cedros Island and the San Benito Islands, Baja California, Mexico, revisited. Geophysical Research Letters 19, 329–332.

Hagstrum, J.T., Murchey, B.L., 1993. Deposition of Franciscan Complex cherts along the paleoequator and accretion to the American margin at tropical paleolatitudes. Geological Society of America Bulletin 105 (6), 766–778.

Hagstrum, J.T., Murchey, B.L., Bogar, R.S., 1996. Equatorial origin for Lower Jurassic radiolarian chert in the Franciscan Complex, San Rafael Mountains, Southern California. Journal of Geophysical Research, B, Solid Earth and Planets 101 (1), 613–626.

Jenkins, H.C., Winterer, E.L., 1982. Paleoceanography of Mesozoic ribbon radiolarites. Earth and Planetary Science Letters 60, 352–375.

Jolivet, L., Goffé, B., Monié, P., Truffert-Luxey, C., Patriat, M., Bonneau, M., 1996. Miocene detachment on Crete and exhumation *P–T–t* paths of high-pressure metamorphic rocks. Tectonics 15, 1129–1153.

Jolivet, L., Facenna, C., Goffé, B., Burov, E., Agard, P., 2003. Subduction tectonics and exhumation of high-pressure metamorphic rocks in the Mediterranean orogen. American Journal of Science 303, 353–409.

Kirschvink, J.L., 1980. The least-squares line and plane and analysis of paleomagnetic data. Royal Astronomical Society of Geophysical Journal 62, 699–718.

Kissel, C., Laj, C., 1988. The tertiary geodynamical evolution of the Aegean arc: a paleomagnetic reconstruction. Tectonophysics 146, 183–201.

Kissel, C., Laj, C., Poisson, A., Simeakis, K., 1989. A pattern of block rotations in central Aegean. In: Kissel, C., Laj, C. (Eds.), Palaeomagnetic Rotations and Continental Deformation. Kluwer Academic Publishers, Dordrecht, pp. 115–129.

Kissel, C., Laj, C., Poisson, A., Görür, N., 2003. Paleomagnetic reconstruction of the Cenozoic evolution of the Eastern Mediterranean. Tectonophysics 362, 199–217.

Kondopoulou, D., 2000. Palaeomagnetism in Greece; Cenozoic and Mesozoic components and their geodynamic implications. Tectonophysics 326 (1–2), 131–151.

Laj, C., Jamet, M., Sorel, D., Valente, J.P., 1982. First paleomagnetic results from Mio–Pliocene series of the Hellenic sedimentary arc. In: Le Pichon, X., Augustithis, S.S., Mascle, J. (Eds.), Geodynamics of the Hellenic Arc and Trench. Tectonophysics, pp. 45–67.

Mauritsch, H.J., Scholger, R., Bushati, S.L., Ramiz, H., 1995. Paleomagnetic investigations in Southern Albanian and their significance for the geodynamic evolution of the Dinarides, Albanides and Hellenides. Tectonophysics 242, 5–18.

McFadden, P.L., Lowes, F.J., 1981. The discrimination of mean directions drawn from Fisher distributions. Royal Astronomical Society of Geophysical Journal 67, 19–33.

McFadden, P.L., McElhinny, M.W., 1990. Classification of the reversal test in paleomagnetism. Geophysical Journal International 103, 725–729.

Morris, A., 1995. Rotational deformation during Palaeogene thrusting and basin closure in eastern central Greece: paleomagnetic evidence from Mesozoic carbonates. Geophysical Journal International 121 (3), 827–847.

Muttoni, G., Channell, J.E.T., Nicora, A., Rettori, R., 1994. Magnetostratigraphy and biostratigraphy of an Anisian–Ladinian (Middle Triassic) boundary section from Hydra (Greece). Palaeogeography, Palaeoclimatology, Palaeoecology 111, 249–262.

Muttoni, G., Kent, D.V., Brack, P., Nicora, A., Balini, M., 1997. Middle Triassic magnetostratigraphy and biostratigraphy from the Dolomites and Greece. Earth and Planetary Science Letters 146 (1–2), 107–120.

Muttoni, G., Erba, E., Kent, D.V., Bachtadse, V., 2005. Mesozoic Alpine facies deposition as a result of past latitudinal plate motion. Nature 434, 59–63.

Pucher, R., Bannert, D., Fromm, K., 1974. Paleomagnetism in Greece: indications of relative block movement. Tectonophysics 22, 31–39.

Richter, D., Mariolakos, I., Risch, H., 1978. The main flysch stages of the Hellenides. In: Closs, H., Roeder, D., Schmidt, K. (Eds.), Alps, Apennines, Hellenides, vol. 38. Inter-Union Commission on Geodynamics Scientific Report, Stuttgart, pp. 434–438.

Ring, U., Layer, P.W., Reischmann, T., 2001. Miocene high-pressure metamorphism in the Cyclades and Crete, Aegean Sea, Greece: evidence for large-magnitude displacement on the Cretan detachment. Geology 29, 395–398.

Robertson, A.H.F., Dixon, K.W., Brown, S., Collins, A., Morris, A., Pickett, E., Sharp, I., Ustaömer, T., 1996. Alternative tectonic models for the Late Paleozoic–Early Tertiary developments of Tethys in the Eastern Mediterranean region. In: Morris, A., Tarling, D.H. (Eds.), Paleomagnetism and Tectonics of the Mediterranean Region. Geologic Society Special Publication, vol. 105, pp. 239–263.

Shibuya, H., Sasajima, S., 1986. Paleomagnetism of red cherts: a case study in the Inuyama area, central Japan. Journal of Geophysical Research 91, 14105–14116.

Surmont, J., 1989. Paléomagnétisme dans les Hellénides internes: analyse des aimantations superposées par la méthode des cercles de réaimantation. Canadian Journal of Earth Sciences 26, 2479–2494.

Turnell, H.B., 1988. Mesozoic evolution of Greek microplates from paleomagnetic measurements. Tectonophysics 155, 307–316.

Van der Voo, R., 1993. Paleomagnetism of the Atlantic, Tethys and Iapetus Oceans. Cambridge University Press, Cambridge. 411 pp.

van Hinsbergen, D.J.J., Langereis, C.G., Meulenkamp, J.E., 2005a. Revision of the timing, magnitude and distribution of Neogene rotations in the western Aegean region. Tectonophysics 396, 1–34.

van Hinsbergen, D.J.J., Hafkenscheid, E., Spakman, W., Meulenkamp, J.E., Wortel, M.J.R., 2005b. Nappe stacking resulting from subduction of oceanic and continental lithosphere below Greece. Geology 33, 325–328.

van Hinsbergen, D.J.J., Zachariasse, W.J., Wortel, M.J.R., Meulenkamp, J.E., 2005c. Underthrusting and exhumation: a comparison between the External Hellenides and the "hot" Cycladic and "cold" South Aegean core complexes (Greece). Tectonics 24, TC2011. doi:10.1029/2004TC001692.

van Hinsbergen, D.J.J., van der Meer, D.G., Zachariasse, W.J., Meulenkamp, J.E., 2006. Deformation of western Greece during Neogene clockwise rotation and collision with Apulia. International Journal of Earth Sciences 95, 463–490.

Winterer, E.L., Bosellini, A., 1981. Subsidence and sedimentation on a Jurassic passive continental margin, Southern Alps, Italy. A.A.P.G. Bulletin 65, 394–421.